Available online at www.sciencedirect.com

SCIENCE DIRECT

Biochimica et Biophysica Acta 1709 (2005) 45 – 57

BIOCHIMICA ET BIOPHYSICA ACTA BBA

http://www.elsevier.com/locate/bba

Improved survival of very high light and oxidative stress is conferred by spontaneous gain-of-function mutations in *Chlamydomonas*

Britta Förster, C. Barry Osmond, Barry J. Pogson*

ARC Centre of Excellence in Plant Energy Biology, School of Biochemistry and Molecular Biology, Bldg. 41, The Australian National University, Canberra, ACT 0200, Australia

Received 14 January 2005; received in revised form 18 May 2005; accepted 24 May 2005
Available online 21 June 2005

Abstract

Investigations into high light and oxidative stress in photosynthetic organisms have focussed primarily on genetic impairment of different photoprotective functions. There are few reports of "gain-of-function" mutations that provide enhanced resistance to high light and/or oxidative stress without reduced productivity. We have isolated at least four such very high light resistant (VHL^R) mutations in the green alga, *Chlamydomonas reinhardtii*, that permit near maximal growth rates at light intensities lethal to wild type. This resistance is not due to an alteration in electron transport rate or quantity and functionality of the two photosystems that could have enhanced photochemical quenching. Nor is it due to reduced excitation pressure by downregulation of the light harvesting antennae or increased nonphotochemical quenching. In fact, photosynthetic activity is unaffected in more than 30 VHL^R isolates. Instead, the basis of the VHL^R phenotype is a combination of traits, which appears to be dominated by enhanced capacity to tolerate reactive oxygen species generated by excess light, methylviologen, rose bengal or hydrogen peroxide. This is further evidenced in lower levels of ROS after exposure to very high light in the VHL^R-*S9* mutant. Additionally, the VHL^R phenotype is associated with increased zeaxanthin accumulation, maintenance of fast synthesis and degradation rates of the D1 protein, and sustained balanced electron flow into and out of PSI under very high light. We conclude that the VHL^R mutations arose from a selection pressure that favors changes to the regulatory system(s) that coordinates several photoprotective processes amongst which repair of PSII and enhanced detoxification of reactive oxygen species play seminal roles.

Keywords: *Chlamydomonas*; High light resistance; Photosynthesis; Photosystem I and II; Photoprotection; Photo-oxidative stress

1. Introduction

High light stress is a determining factor for productivity and survival of photosynthetic organisms. Hence, at any irradiance level, photosynthetic competence and efficiency reflect the balance of photoprotective and photorepair mechanisms against photoinactivation and photodamage. Acclimation to high light obviously requires coordinated and well-balanced adjustments in the photosynthetic apparatus [1] to cope with the increased excitation pressure and greater need for photoprotection. Typically, high light acclimation involves downsizing of the antennae and both photosystem I (PSI) and II (PSII), while levels of zeaxanthin, antioxidants, scavenging systems for reactive oxygen species (ROS) and photorepair mechanisms such as turnover of the D1 protein of PSII are increased. Furthermore, changes in the PSII-PSI stoichiometry and in carbon assimilation can be commonly observed in vascular plants as well as in cyanobacteria and algae. In eukaryotic photosynthetic organisms, these adjustments to high light environments require differential chloroplast and nuclear

Abbreviations: Chl, chlorophyll; D1, D1 reaction center protein; DPS, de-epoxidation state of xanthophyll cycle pigments; DAB, 3,3′diaminobenzidine; F_o and F_m, minimum and maximum fluorescence; F_v/F_m, maximum dark-adapted efficiency of photosystem II; Lhcp, light harvesting complex protein; MV, methylviologen; NBT, nitroblue tetrazolium; NPQ, nonphotochemical quenching of chlorophyll fluorescence; PSI, photosystem I; PSII, photosystems II; ROS, reactive oxygen species; VHL^R, very high light resistant mutations

* Corresponding author. Tel.: +61 2 61255629; fax: +61 2 61250313.
E-mail address: barry.pogson@anu.edu.au (B.J. Pogson).

0005-2728/$ - see front matter © 2005 Elsevier B.V. All rights reserved.
doi:10.1016/j.bbabio.2005.05.012

gene expression that may be controlled by the redox state of chloroplast components, carbon metabolism and/or ROS. However, specific signalling molecules and signal transduction cascades are not well understood.

The light-harvesting antennae consist of chlorophyll and carotenoid pigment–protein complexes that absorb photons and deliver excitation energy to PSII and PSI, but can also dissipate excitation energy as heat. The increased de-epoxidation state (DPS) of the xanthophyll cycle pigments in high light plays a major protective role and is often correlated with induction of nonphotochemical fluorescence quenching (NPQ) [2,3]. Evidently, the photoprotective roles of xanthophylls are not limited to NPQ. An important example is zeaxanthin which also provides enhanced protection against lipid peroxidation [4,5].

Maintenance of PSII structure and function is crucial to survival under high irradiances because PSII, particularly the D1 protein, is a primary target of photoinactivation [1,6]. The state of PSII electron transfer and redox reactions seems to control susceptibility to photodamage [7], which is usually exacerbated if PSII becomes over-reduced under high excitation pressure. Although damaged PSII centers can also exert a form of photoprotection in higher plants [8], the majority of inactivated PSII centers are usually repaired with de novo synthesized D1 protein [6].

Changes in PSI function may also alter photosensitivity. PSI-deficient cyanobacteria or algae cannot grow photoautotrophically, and deleterious mutations in PSI usually enhance sensitivity to high light [9]. However, PSI is rarely the primary site of photoinhibition because PSII is normally more susceptible to photoinactivation in high light [10]. Furthermore, photoinhibition is directly correlated with singlet oxygen ($^1O_2^*$) production in photoinactivated PSII centers [11], whereas no production of $^1O_2^*$ was found in PSI under photoinhibitory conditions [12]. It has been proposed that P700 is shielded from oxygen, as the decay of the P700 triplet state in PSI particles is essentially unaffected by the presence of O_2, which indicates that the formation of $^1O_2^*$ in PSI is rather an unlikely event [13]. Moreover, Barth et al. showed that oxidized P700 accumulates under high light stress and suggested that this cation radical dissipates excitation energy as heat, thus contributing to stabilization of PSI [10]. Therefore, redox balance of the photosynthetic electron transport chain, so widely implicated in control of gene expression [14], seems to be primarily determined by PSII activities. Nonetheless, PSI activity can also modulate the redox state of the chloroplast as the ratio of NADPH to ATP generation and the re-reduction of the intersystem Cytochrome b_6f complex can be adjusted by switching between linear and cyclic electron flow [15,16].

Reactive oxygen species are generated as inevitable by-products of the photosynthetic reactions in both PSII and PSI [14,17,18]. Increased accumulation of excitation energy in the antenna complexes in high light favors formation of triplet excited state chlorophylls (^{3}Chl) that can directly interact with O_2 to form reactive singlet oxygen. Additionally, highly reduced photosynthetic electron carriers would enhance reduction of O_2 by PSI, which leads to subsequent formation of superoxide anions (O_2^-), hydroxyl ($^{\bullet}$OH) radicals and hydrogen peroxide (H_2O_2). ROS readily cause oxidative damage to membrane lipids, proteins and nuclear acids and ultimately death of the cell. Several ROS scavenging mechanisms operate in chloroplasts and throughout cells including enzymatic reactions such as superoxide dismutases, catalases, ascorbate peroxidases (APX) and antioxidants such as zeaxanthin, α-tocopherol, ascorbate and glutathione that both directly detoxify ROS and contribute to specific enzymatic reactions [3,19]. Taken together, alterations in any one or more of these acclimatory and protective processes could determine whether photosynthetic organisms survive and grow under high light and other lethal oxidative stress conditions.

High light stress responses have been examined in many mutants that show increased susceptibility to photoinactivation under high irradiances [2,3,20,21]. Few mutants have been identified that showed enhanced tolerance to high irradiances [22], and tolerance is more typically due to overexpression of endogenous or foreign transgenes [23,24] or inhibition of one photoprotective process has led to upregulation of another [25], indicating a level of regulation above changes in structural genes. However, to date, there have been few reports of unequivocal "gain-of-function mutations" that permit near normal growth rates under lethal intensities of high light. Consequently, it is not well understood how the coordinated regulation of response pathways to light stress is controlled.

Very high light resistant (VHL^R) mutants of the green alga *Chlamydomonas reinhardtii* represent such a rare gain-of-function due to mutation in nuclear genes. Previous analysis of VHL^R strains has shown that mutants selected from wild type express high levels of both NPQ and zeaxanthin, whereas those selected from a strain with decreased PSII electron transport generate high zeaxanthin levels but lack the ability to significantly induce NPQ [26]. This is additional support for the general concept of multiple protective roles of zeaxanthin that need to be considered further in these mutants. It has also been found that acceptor sides of PSII centers are unexpectedly highly reduced in the VHL^R mutants under high irradiances [26], which should enhance the probability for photoinactivation and photodamage.

In this context, it seems probable that VHL^R mutants are altered in one or more of the aforementioned photoprotective and photorepair processes, thereby conferring greater capacity to manage excess light levels. Thus, we have systematically analyzed the abundance and activities of the major components of the photosynthetic electron transport system in VHL^R mutants including amounts of key photosystem proteins, chlorophyll, and functional PSII and PSI reaction centers. Moreover, D1 protein synthesis and degradation were analyzed to assess the potential for PSII

repair, and electron transfer to and from the PSI reaction center (P700) was investigated to better understand implications for the probability of energy transfer to alternative acceptors involved in ROS generation in excess light. Additionally, we determined the level of ROS under various light conditions and investigated the tolerance of *VHL*^{R} mutants to different oxidative stresses.

2. Materials and methods

C. reinhardtii wild type CC-125 was obtained from the *Chlamydomonas* Genetics Center (Dr. E. Harris, Duke University, USA). The *L** parent strain (CC-3376) and *VHL*^{R} mutants *VHL*^{R}*-S9*, *VHL*^{R}*-S4*, *VHL*^{R}*-L4*, *VHL*^{R}*-L30* were isolated as reported [27] and illustrated in Fig. 1. Crosses and allelism tests were carried out as described [28]. For physiological analyses, cells were grown at 25 °C with liquid minimal HS media, agitated and bubbled with 5% CO_2 enriched air in continuous low light (LL, 70 μmol photons m^{-2} s^{-1}), high light (HL, 600 μmol photons m^{-2} s^{-1}), or very high light (VHL, 2000 μmol photons m^{-2} s^{-1} and 1500 μmol photons m^{-2} s^{-1} used for strains with the *L** mutation). For light shift experiments, HL acclimated cultures were transferred to VHL for up to 24 h. For ROS assays, cells were grown with HS medium in LL or HL and bubbled with air.

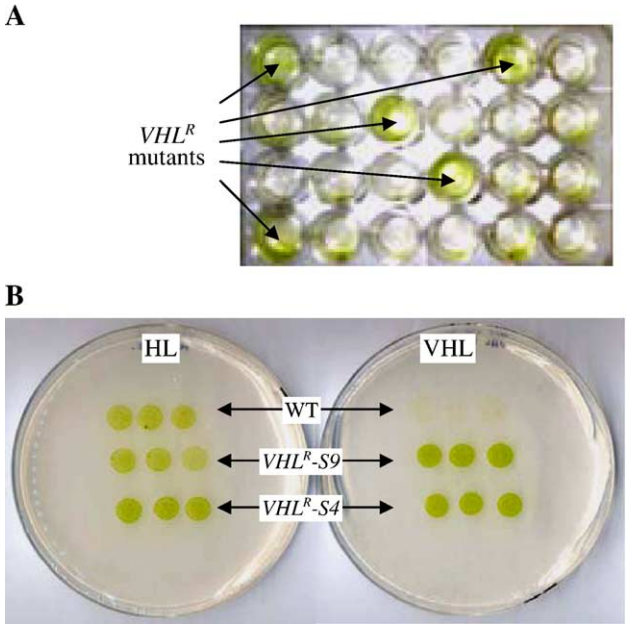

Fig. 1. Selection and growth of *VHL*^{R} mutants. (A) Photoautotrophic cell suspension cultures of wild type CC-125 grown in HL were transferred to continuous VHL. Cells bleached and died during week 1 and 2 in VHL (clear or faintly-yellow cultures) and individual cultures re-greened due to growth of spontaneously arising *VHL*^{R} mutants in week 3. (B) Spot test growth analysis for *VHL*^{R} mutants and wild type. 10 μl spots of dilute cell suspensions were incubated for 9 days in permissive HL or in selective VHL.

Total biomass (A_{750}) was determined as optical density of cell suspensions in a spectrophotometer at 750 nm. The A_{750} values from 0.01 to 0.9 are linearly correlated with the cell number in suspension cultures (data not shown). The correlation is not affected by the genotypes or growth condition used in this study indicating that the average cell size has not significantly changed. Total chlorophyll $a+b$ pigments were determined spectrophotometrically in 80% acetone extracts [29]. Functional absorption cross-sections of PSII were calculated from induction curves of maximum fluorescence, which were generated by applying subsaturating short blue light flashes at high frequency with the fast repetition rate fluorometer as described previously [30].

Total proteins were extracted, quantified, separated by denaturing gel electrophoresis and immunoblotted as described [31,32]. 20 μg of total protein extracts were loaded onto the gel for each sample. D1, Lhcp and PsaF proteins were quantitatively detected by chemiluminescence using polyclonal antisera that were kindly provided by Drs. P. B. Heifetz, B. D. Kohorn and W. Zerges (Duke University, N.C., USA), respectively.

Pulse-chase labeling experiments of chloroplast proteins followed described methods [31–33]. D1 protein synthesis rates were deduced from linear increase of ^{35}S incorporation into protein in sulphate-starved cells for 20 min. Half-life times of degradation ($t_{1/2}$) were calculated from exponential decay of labeled protein over 120 min after adding the protein synthesis inhibitors anisomycin (Pfizer) and lincomycin (Sigma).

Amounts of functional PSII centers were estimated from O_2 flash yields [34] in cell suspensions using a modified Hansatech O_2 measuring system [21] fitted with white strobe lights to deliver single turnover flashes. Different flash frequencies (maximum 40 Hz) were used to determine O_2 evolution/flash in the linear phase before saturation of O_2 evolution. It was assumed that evolution of one molecule of O_2 requires turnover of four PSII centers. Maximum efficiency of dark-adapted PSII centers ($F_v/F_m=(F_m-F_o)/F_m$) was determined from chlorophyll fluorescence in cell suspensions with a pulse-amplified modulation fluorometer (PAM101, Walz, Effeltrich, Germany) [26,27] and from cell cultures spotted onto agar plates with a fluorescence imaging system (FluorCam 700MF, Photosystem Instruments, Brno, Czech Republic).

Amounts of active PSI centers and P700 oxidation and reduction kinetics were estimated from saturating far red light (715±15 nm) induced absorbance changes at 800–830 nm (A_{800}) due to $P700^+$ formation using a PAM 101 fluorometer equipped with an ED800-T emitter-detector unit. Cell suspensions were filtered onto glass fiber filters (diameter 24 mm, GF/C, Whatman), moistened with 100 μl HS minimal medium containing 10 mM Na-bicarbonate and positioned immediately under the fiberoptic. $P700^+$ re-reduction was determined from reversal of the far red light induced A_{800} signal in the dark.

Resistance to exogenously applied ROS-generating reagents rose bengal (Sigma) and methylviologen (MV; Sigma), and H_2O_2 (BDH) was measured by adapting the herbicide resistance assay described in [35], and biomass was determined in 1 ml cell suspension cultures distributed across 24-well microtiter plates after 72 or 96 h in LL and in HL. Singlet oxygen was increased by RB, superoxide by MV and additional H_2O_2 was supplied directly from 100-fold concentrated stock solutions. Concentrations of MV, RB or H_2O_2 in the medium causing 50% inhibition of growth (I_{50}) were derived from line plots of the normalized relative A_{750} values over the series of concentration tested. The A_{750} value of the water-treated control culture of each genotype was chosen as 100% reference value for each experiment. I_{50} values were averaged and statistical significances evaluated at 95% confidence level ($p<0.05$) using XLSTAT© software (Addinsoft) for multiple and pairwise comparison analysis of variance (ANOVA).

Levels of cumulative O_2^- production were evaluated based on in vivo staining of LL and HL grown photoautotrophic cell suspensions with nitroblue tetrazolium (NBT; Sigma). H_2O_2 levels were determined by in vivo staining with 3,3′diaminobenzidine (DAB)–HCl (Sigma). Equal amounts of biomass (total $A_{750}=2$) from log phase cell cultures were filtered onto glass microfiber filters (diameter 24 mm, GF/C; Whatman), moistened with 200 μl minimal medium containing 1 mM NBT or 5 mM DAB and subsequently incubated either at LL for 40 min or exposed to VHL for 10 min up to 1 h. Chlorophylls and carotenoid pigments were completely extracted following 10 min incubation of the filter discs in 2 ml 80% acetone at 20 °C. NBT is directly reduced by O_2^-, which generates the water-insoluble, deep blue formazan precipitate. DAB interacts with H_2O_2 generating a reddish-brown polymerization product. Staining was compared semi-quantitatively between different cell lines on the filter discs after removal of pigments. Filters were scanned as digital images from which staining intensities were estimated by densitometry.

3. Results

We established previously that the *VHL*^{R} mutations are nuclear mutations. They were isolated as spontaneous mutations in two different genetic backgrounds, i.e., from wild type or from the photosynthetically impaired *L** strain [27] (Fig. 1). *L** is a site-directed mutant with an Ala to Leu substitution at position 251 in the D1 protein that decreases PSII electron transfer from Q_A to Q_B and confers resistance to herbicides targeting the Q_B binding site in PSII [32,35]. The four *VHL*^{R} mutants analyzed in detail in this work, i.e., two isolates from wild type (*VHL*^{R}*-S9*, *VHL*^{R}*-S4*) and two *VHL*^{R}*-L** isolates (*VHL*^{R}*-L4*, *VHL*^{R}*-L30*) from *L**, are shown to be non-allelic (Table 1). In a haploid organism such as *Chlamydomonas*, crosses of non-allelic *VHL*^{R} mutations would result in both sensitive and resistant progeny in F1 population. Therefore, the occurrence of VHL sensitive progeny from each cross proves these are four different *VHL*^{R} loci.

Table 1
Analysis of allelism in four *VHL*^{R} mutants

Parental cross	% *VHL*^{S}	*VHL*^{S}	*VHL*^{R}	Total progeny
S9 × S4	52	28	26	54
L4 × L30	77	43	13	56
S4 × L4	47	20	23	43
S4 × L30	65	44	24	68
S9 × L4	37	10	17	27
S9 × L30	43	20	10	30

Reciprocal crosses between *VHL*^{R}*-S4, VHL*^{R}*-S9, VHL*^{R}*-L4 and VHL*^{R}*-L30* were performed to identify VHL sensitive (*VHL*^{S}) F1 progeny resulting from crosses of non-allelic *VHL*^{R} loci.

Size and structure of the light-harvesting antennae modulate both light absorption and energy transfer as well as thermal dissipation of excess photons. Changes in the antennae were examined based on the accumulation of three light-harvesting complex proteins (Lhcp; apparent molecular weights 25, 26 and 29 kDa) and total chlorophyll *a*+*b* (Chl) contents (Fig. 2). For comparison, Lhcp and total Chl levels were normalized to the total biomass units of the samples (Fig. 2B). Not surprisingly, wild type acclimated to HL by reducing antenna proteins and pigment to about 50% of LL levels. However, the Chl *a*/*b* ratio did not increase significantly in HL indicating that the ratio of peripheral antennae to photosystem core complexes was relatively similar to the ratio in LL. Since exposure of wild type or *L** to excess light for several days is lethal, these strains could only be studied by transfer of HL-acclimated cell cultures to VHL for no longer than 24 h. Following the shift to VHL, Lhcps declined to 1% and Chl to 20% of LL levels, whether expressed in terms of protein (Fig. 2A) or biomass (Fig. 2B). The concomitant increase in Chl *a*/*b* ratio in VHL is consistent with the increased loss of peripheral antennae relative to photosystem core complexes. *VHL*^{R}*-S9* had similar Lhcp levels as WT and maintained slightly higher Chl levels in LL and HL. The striking difference, however, is in very high light, where *VHL*^{R}*-S9* maintained 10-fold higher Lhcp levels and twice the Chl content of wild type. In spite of some substantial changes in Lhcp and Chl levels in response to different light conditions, functional absorption cross sections of PSII (σ_{PSII}) were unchanged (Fig. 2B). A similar comparison of the very high light sensitive parent *L** and its resistant progeny *VHL*^{R}*-L4* revealed that the resistance does not correlate with adjustments of antenna sizes and functional absorption cross sections of PSII (Fig. 2C, D). In the VHL sensitive *L** the Lhcps or Chl did not decline below 50% of LL levels, and Lhcp and Chl levels did not differ from *VHL*^{R}*-L4* at any light intensity even though *L** dies after approximately the same time as wild type in VHL.

The D1 protein pool sizes (Fig. 3A) are representative of the total amount of fully assembled PSII centers since there is one D1 subunit per reaction center, and mature size

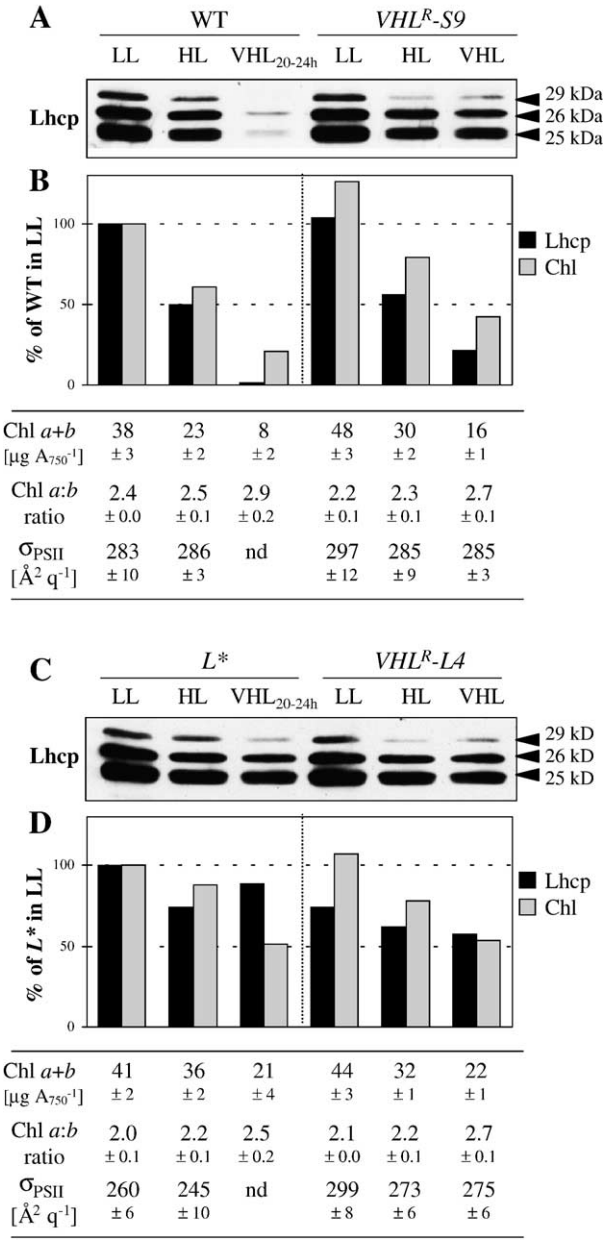

	WT LL	WT HL	WT VHL$_{20-24h}$	*VHL^R-S9* LL	*VHL^R-S9* HL	*VHL^R-S9* VHL
Chl *a*+*b* [µg A_{750}^{-1}]	38 ± 3	23 ± 2	8 ± 2	48 ± 3	30 ± 2	16 ± 1
Chl *a*:*b* ratio	2.4 ± 0.0	2.5 ± 0.1	2.9 ± 0.2	2.2 ± 0.1	2.3 ± 0.1	2.7 ± 0.1
σ_{PSII} [Å^2 q^{-1}]	283 ± 10	286 ± 3	nd	297 ± 12	285 ± 9	285 ± 3

	WT LL	WT HL	WT VHL$_{20-24h}$	*VHL^R-L4* LL	*VHL^R-L4* HL	*VHL^R-L4* VHL
Chl *a*+*b* [µg A_{750}^{-1}]	41 ± 2	36 ± 2	21 ± 4	44 ± 3	32 ± 1	22 ± 1
Chl *a*:*b* ratio	2.0 ± 0.1	2.2 ± 0.1	2.5 ± 0.2	2.1 ± 0.0	2.2 ± 0.1	2.7 ± 0.1
σ_{PSII} [Å^2 q^{-1}]	260 ± 6	245 ± 10	nd	299 ± 8	273 ± 6	275 ± 6

Fig. 2. Comparison of the amounts of light-harvesting antennae protein (Lhcp), chlorophyll (Chl) pigments and functional antenna sizes in wildtype (WT) and *VHL^R-S9*, and *L** and composite data of isolates *VHL^R-L4* and *VHL^R-L5* under LL, HL and VHL. (A, C) Western blots showing accumulation of three Lhc proteins (25, 26 and 29 kDa) are representative of at least 2 other replicates. (B, D) Total Lhcp contents corrected for biomass A_{750} (black columns) were compared to average total Chl *a*+*b* content per A_{750} (grey columns). Values are plotted as the percentage of WT (B) or *L** (D) grown in LL. Corresponding absolute amounts of Chl *a*+*b* normalized to biomass, Chl *a*/*b* ratios and the average functional absorption cross-sections of PSII (α_{PSII}) are shown in the tables below the plots. Values are means ± standard error of n = 5–10 experiments; nd, not determined.

protein is thought to accumulate only when it is integrated into PSII reaction centers. However, it remains elusive whether these PSII centers are functional. Therefore, the amount of active PSII centers was deduced from O_2 flash yield measurements. The amounts of fully assembled PSII centers and functional, O_2-evolving PSII centers were compared relative to the levels in wild type in LL after normalization to biomass (Fig. 3B). Wild type and *VHL^R-S9* had similar levels of D1 protein in LL, which declined in HL and decreased further in VHL to 25% of LL levels. The number of functional PSII centers, on the other hand, remained the same in *VHL^R-S9* in LL and HL and decreased moderately in VHL, whereas wild type showed the same large decrease in functional PSII as observed for D1. This suggests that the smaller total PSII pools under high light had a relatively higher proportion of active PSII centers in *VHL^R-S9* but not in wild type. Moreover, the observation that a relatively large decrease in D1 protein in *VHL^R-S9* in HL and VHL corresponds to a relatively small decrease in functional PSII centers may indicate a proportion of the detectable D1 protein is inactive. However, the fact that strains carrying the additional *L** mutation had little decrease in D1 protein or functional PSII centers at any light intensity implies that alterations in functionality and amounts of active PSII centers are not the origin of the *VHL^R* phenotype. This is further corroborated by the fact that the 23 *VHL^R* mutants isolated from wild type (*VHL^R-S*) do not differ from the strain of origin in PSII functionality, evident from dark-adapted F_v/F_m in HL and following 24 h transfer to VHL (Fig. 4A, B). Likewise, 9 *VHL^R* mutants from *L** (*VHL^R-L**) show similar F_v/F_m values as the original *L** strain in HL and after 24 h in VHL.

The D1 protein pool sizes in *VHL^R* mutants and parent reflect the result of the dynamic interaction of protein

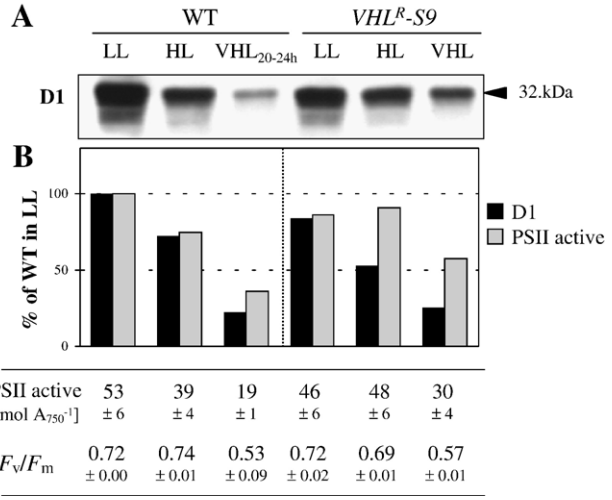

	WT LL	WT HL	WT VHL$_{20-24h}$	*VHL^R-S9* LL	*VHL^R-S9* HL	*VHL^R-S9* VHL
PSII active [pmol A_{750}^{-1}]	53 ± 6	39 ± 4	19 ± 1	46 ± 6	48 ± 6	30 ± 4
F_v/F_m	0.72 ± 0.00	0.74 ± 0.01	0.53 ± 0.09	0.72 ± 0.02	0.69 ± 0.01	0.57 ± 0.01

Fig. 3. D1 protein pool size and amounts of functional PSII centers. (A) Western blots showing accumulation of the mature 32.5 kDa D1 protein. Similar results were obtained in two more replicates. (B) Amounts of D1 protein corrected for biomass A_{750} corresponding to the total protein loaded for each sample (black columns) were compared to amounts of functional PSII reaction centers per A_{750} (grey columns). Values are plotted as percentage of WT in LL. Corresponding absolute amounts of functional PSII normalized to biomass and maximum dark-adapted efficiency of PSII (F_v/F_m) are in the table below the plot. Values are means ± standard error of n = 4–16 experiments.

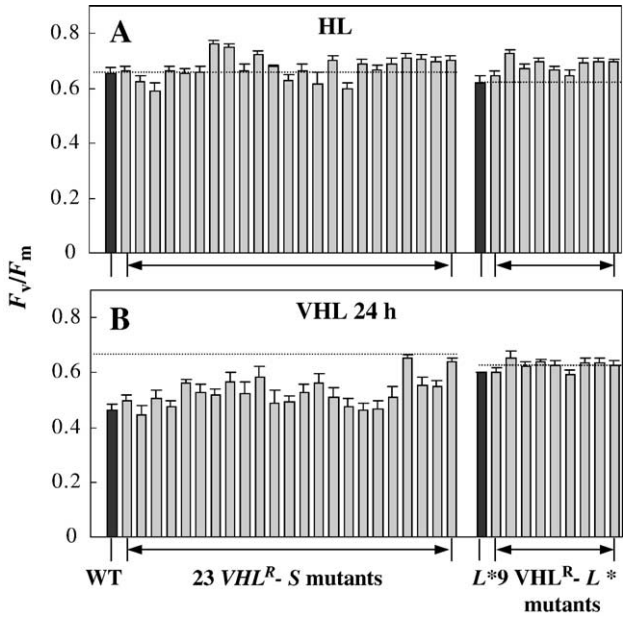

Fig. 4. Comparison of PSII activity in *VHL*^{R} mutants derived from wild type (WT) and *L**. Fluorescence imaging was used to determine the maximum dark-adapted PSII efficiencies (F_v/F_m) of 23 *VHL*^{R} mutants, isolated from WT (*VHL*^{R}-*S*) and 9 mutants from *L** (*VHL*^{R}-*L**) in HL (A) and after 24 h exposure to VHL (B). WT and *L** are represented as black columns, *VHL*^{R}-mutants as grey columns. The dashed lines indicate the average F_v/F_m of WT and *L** in HL. Values are means ± standard error of at least $n=3$ experiments.

synthesis and degradation. Consequently, synthesis and degradation rates were investigated separately using pulse-chase labeling in HL and VHL (Fig. 5). Protein synthesis rates represent the balance of ^{35}S label incorporation and any simultaneous loss due to continuing protein degradation as it is technically not feasible to block degradation without disturbing the rate of synthesis. Thus, it is the apparent or net synthesis rate that is measured during the pulse, which underestimates the actual protein synthesis rates depending on how fast concomitant degradation occurs. In Fig. 4A, it is shown that the D1 protein is synthesized at the same net rate when wild type and *VHL*^{R}-*S9* are grown in HL, whereas after 20 h in very high light, the net rate of synthesis is 2.5-fold higher in *VHL*^{R}-*S9* than in wild type.

Following ^{35}S labeling of de novo synthesized D1 protein, degradation rates and half-life times were measured directly from loss of label, while synthesis was completely blocked with specific protein synthesis inhibitors (Fig. 5B). In HL, the half-life of the D1 protein was about 2 times shorter in *VHL*^{R}-*S9* than in wild type. Similar observations were made comparing *L** and *VHL*^{R}-*L4* in HL which revealed slightly faster synthesis of D1 as well as faster degradation in *VHL*^{R}-*L4*, comparable to *VHL*^{R}-*S9*. Exposure to very high light for 20 h had little effect on the rate of D1 degradation in *VHL*^{R}-*S9*, whereas in wild type, D1 was degraded twice as fast as in HL. Combined, the relative differences in net synthesis and degradation reveal that wild type is essentially unable to compensate for the faster D1 degradation after 20 h in excess light by increasing synthesis accordingly. While losing D1 as fast as *VHL*^{R}-*S9*, synthesis is 2.5-fold slower in wild type, which, although not fully reflected in total D1 pool size and PSII function at that time (Fig. 3), may be a sign of already decreasing viability.

Amounts of PSI centers were estimated from the levels of the PsaF subunit of the PSI complex with the assumption that PsaF, which facilitates plastocyanin docking and fast electron transfer to PSI, normally accumulates stoichiometrically. PsaF levels decreased with higher light to a very similar extent as observed for the D1 protein and the Lhcps with about 25% of LL levels present in very high light. Almost no differences were observed in PsaF levels between wild type and *VHL*^{R}-*S9* regardless of normalization to total protein or biomass (Fig. 6A, B). The relative amounts of functional PSI centers were determined from far red light induced absorbance changes at 800 nm (A_{800}), which correlate with formation of oxidized PSI ($P700^+$). Functional PSI centers decrease in a light dependent manner in parallel with PsaF. Interestingly, *VHL*^{R}-*S9* retains significantly more functional PSI centers in very high light than wild type but even fewer than the light sensitive *L** strain (data not shown).

Electron transfer to and from the PSI reaction center was calculated from the rates of changes in the A_{800} signal. Oxidation rates of P700 to $P700^+$ were compared to reduction of $P700^+$ to P700 (Fig. 7). The P700 oxidation/reduction ratios are near one in all strains regardless of light levels, which implies that overall the redox state of PSI is not affected. The rates of oxidation and reduction in wild type decreased strongly with increased light intensities, slowing after transfer to very high light to about 10% of the respective LL rates. This trend was not as apparent in *VHL*^{R}-*S9*, especially in VHL, where there was little decline in either the rate of oxidation or reduction of PSI compared to HL rates. However, the equivalent analysis of *L** and *VHL*^{R}-*L** demonstrated that *L** maintains the same fast rates as *VHL*^{R}-*L** and *VHL*^{R}-*S9*. This means again, that light sensitive and *VHL*^{R} strains share the same properties, which discounts differences in levels or function of PSI as the basis for the *VHL*^{R} phenotype.

Growth in the presence of ROS-generating rose bengal (increased $^1O_2^*$), methylviologen (increased O_2^-) or following direct addition of H_2O_2 was measured in LL and in HL. Each of the treatments should lead to the generation of higher intracellular levels of a range of ROS in addition to the levels normally generated in photosynthetically active cells. The linear dose–response curves (Fig. 8) show the means of up to ten experiments of relative biomass accumulation for wild type, *VHL*^{R}-*S9* and *VHL*^{R}-*S4*. The average inhibitor concentrations causing 50% reduction of biomass (I_{50}) deduced from these experiments is reported for all six genotypes evaluated in this study (Table 2). Linear dose response curves and the I_{50} values showed that *VHL*^{R}-*S9* and *VHL*^{R}-*S4* were viable in 2–3 times higher rose bengal concentrations than wild type both in LL (Fig. 8B)

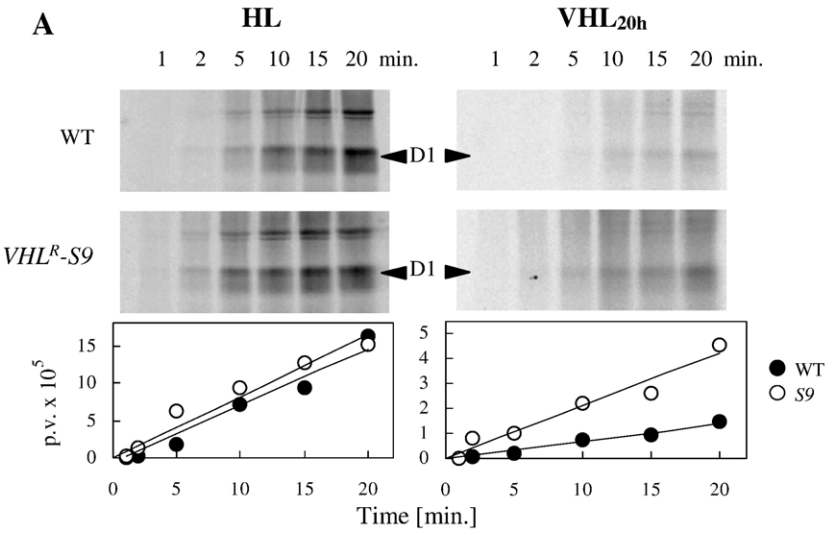

D1 synthesis rates	[%]	[%]
VHL^R*-S9* : WT	99 ± 2	250 ± 8
VHL^R*-L4* : *L**	123 ± 4	nd

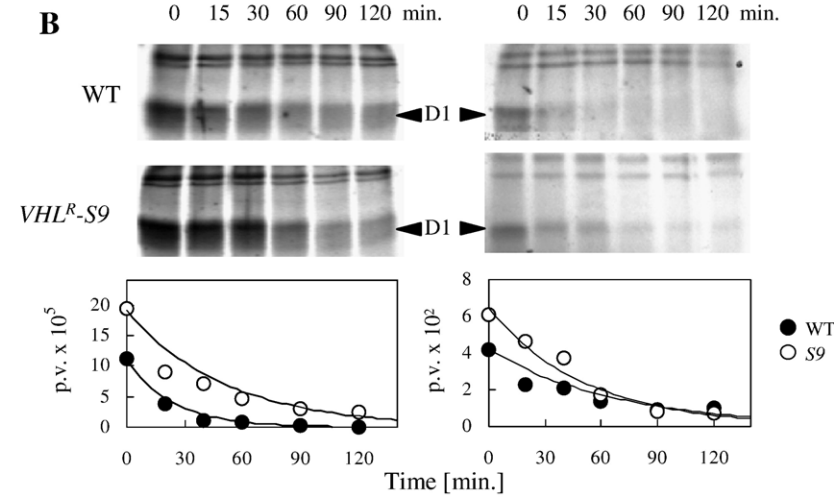

D1 degradation	$t_{1/2}$ [h]	% of WT HL	$t_{1/2}$ [h]	% of WT HL
WT	3.5 ± 0.3	100	1.8 ± 0.1	51
VHL^R*-S9*	1.9 ± 0.2	54	1.6 ± 0.1	46
*L**	2.6 ± 0.3	75	nd	nd
VHL^R*-L4*	1.7 ± 0.2	49	nd	nd

Fig. 5. De novo synthesis and degradation of the D1 protein calculated from ^{35}S pulse-chase labeling of chloroplast proteins. The predominant band at 32–34 kDa was previously confirmed as the D1 protein by immunoprecipitation [21]. Equal amounts of cells were removed at each time point of (A) the synthesis measurement (pulse) and (B) the degradation measurement (chase), and the amount of radioactively-labeled D1 protein (pixel volumes) in the samples was determined from autoradiography. The top of each panel shows representative autoradiograms of wild type (WT) and *VHL*^{R}*-S9* in HL (left) and after 20 h VHL exposure (right) with the corresponding average pixel volumes plotted over time below. Relative synthesis rates plus relative and absolute degradation are shown for WT and *VHL*^{R}*-S9* as well as for *L** and *VHL*^{R}*-L4* in the tables below the plots. The pulse experiment detects newly-synthesized D1 protein. D1 synthesis rates were calculated from linear regression of pixel volumes (p.v.) plotted over time. Following the pulse, chloroplast and cytosolic protein synthesis were inhibited and the ^{35}S label removed to initiate the chase which determines amounts of remaining radioactively-labeled D1 protein at various time points. Exponential decay functions were used to determine the D1 degradation rates and half-life times from pixel volumes plotted over time. Averages are based on 2–6 experiments. nd, not determined.

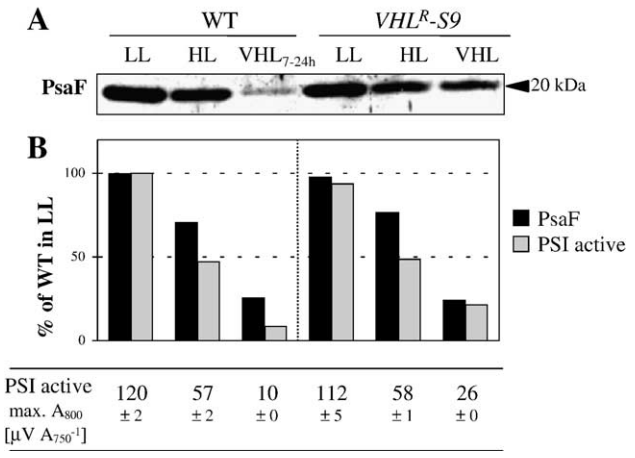

Fig. 6. Accumulation of the PsaF subunit of PSI and amounts of functional PSI centers. Functional PSI centers were defined by their ability to oxidize their reaction center chlorophylls (P700) in response to PSI-specific far red light. (A) Western blot of the 20-kDa PsaF protein. (B) Amounts of PsaF protein corrected for biomass A_{750} (black columns) were compared to amounts of functional PSI reaction centers per A_{750} (grey columns). Values were plotted as percentage of WT in LL. The corresponding absolute A_{800} signal (µV) normalized to biomass is given in the table below the plot. Values are means ± standard error of $n = 6-21$.

and in HL (Fig. 8A, E). The two *VHL*^{R} mutants were similarly resistant to approximately 2–3 times higher concentrations of methylviologen in HL (Fig. 8F, Table 2), whereas MV tolerance was less pronounced and only 1.5–2 times higher in LL (Fig. 8C, Table 2). Resistance (I_{50}) of *VHL*^{R}*-S9* and *VHL*^{R}*-S4* to H_2O_2 differed as it was clearly higher (2 times) relative to wild type (Fig. 8D, Table 2) in LL but showed a marginal, insignificant increase in the I_{50} values in HL. However, the overall HL dose–response curves show a consistent trend to elevated H_2O_2 resistance in both *VHL*^{R} strains (Fig. 8G). Generally, wild type appears to be less sensitive to RB, MV and H_2O_2 in LL with regard to minimal lethal concentrations (Fig. 8), whereas *VHL*^{R}*-S9* and *VHL*^{R}*-S4* do not show a similar dependency on light intensity. Likewise, growth responses of the mutants are largely independent of the light level at sublethal concentrations (compare Fig. 8B and E, C and F, D and G) and show the most markedly increased tolerance to $^1O_2^*$ generated by rose bengal. The two *VHL*^{R}*-L** mutants were also more ROS resistant than their parental strain, *L**, in 4 of the 6 experimental treatments (Table 3). Thus, all four *VHL*^{R} mutations confer enhanced capacity to cope with artificially elevated ROS.

To understand whether the VHL resistance phenotype of different *VHL*^{R} mutants is directly reflected in largely varying levels of intracellular ROS, the superoxide anion and H_2O_2 levels were evaluated in wild type compared to mutants under light stress conditions using the colorigenic NBT and DAB detection assays, respectively (Fig. 9A, B). As it is not always apparent whether the increased ROS levels are the cause or the result of photobleaching and cell death, cells were treated for only 10 min and 1 h with very high light, which does not cause any visible photobleaching in wild type. A common observation for all genotypes was that both O_2^- and H_2O_2 accumulate at higher levels in response to light shift experiments to VHL. Staining with NBT revealed no apparent differences in comparisons of *VHL*^{R}*-S9*, *VHL*^{R}*-S4* and wild type in O_2^- accumulation in LL and HL grown cells (Fig. 9A). However, *VHL*^{R}*-S9* accumulates noticeably less O_2^-, i.e., 50–80% of wild type levels, after 10 min and 1 h exposure to VHL (Figs. 9A4, 5A–B). In contrast, there is no obvious difference in O_2^- levels in *VHL*^{R}*-S4* compared to wild type (Fig. 9A) or the two *VHL*^{R} cell lines carrying the *L** mutation in most of these light treatments (data not shown). Similarly, staining with DAB did not detect genotype specific differences in H_2O_2 accumulation in LL and HL grown cells (Fig. 9B). There is a limited decrease of H_2O_2 levels in *VHL*^{R}*-S9* and *VHL*^{R}*-S4* after 1 h exposure to VHL. The short exposure to VHL is insufficient to cause death of wild type cells, so that higher levels of ROS in wild type compared to *VHL*^{R} mutants are likely to reflect the increased capacity to immediately quench or limit accumulation of ROS in the mutants as opposed to elevated ROS in wild type due to cell death.

4. Discussion

The notion that *VHL*^{R} mutations affect genes at a regulatory level, representing "master switches" for coordinated expression of high light acclimation and photoprotection, is consistent with several observations from studies with other photosynthetic organisms. Thus, far changes in expression of structural genes, e.g., over-

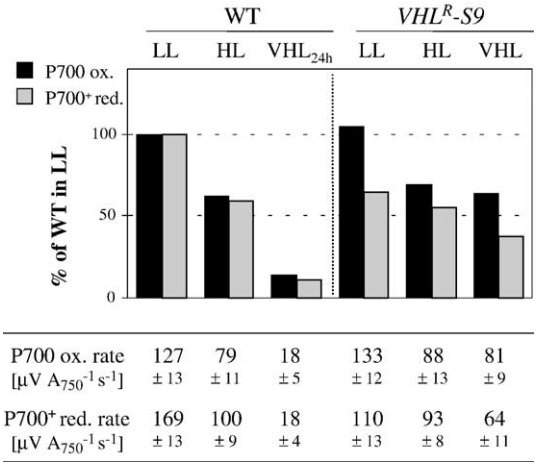

Fig. 7. Electron transfer rates to and from PSI were determined from the A_{800} absorbance changes in intact cells. The rate of P700 oxidation is derived during far red illumination of dark-adapted cells, the re-reduction rate of $P700^+$ after transition from far red light to dark. The balance of these rates is an indirect indication for the redox state of PSI. Oxidation (black columns) and reduction (grey column) rates were plotted as percentage of WT grown in LL. Values are means ± standard errors of $n = 6-21$ experiments.

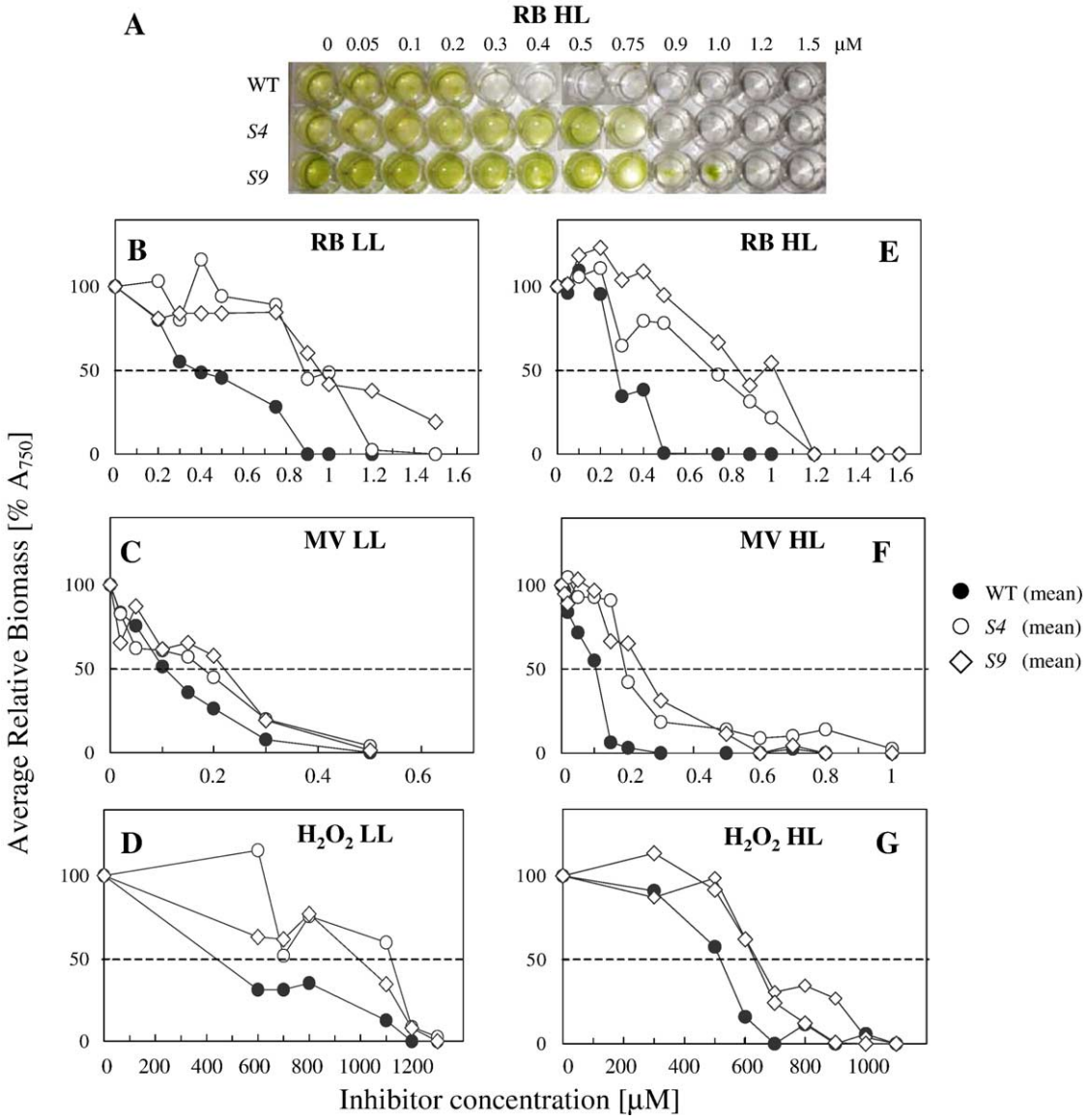

Fig. 8. Resistance to ROS determined from growth assays. Singlet oxygen ($^1O_2^*$) and superoxide (O_2^-) levels were increased indirectly by adding rose bengal (RB) or methylviologen (MV), respectively, whereas additional hydrogen peroxide (H_2O_2) was supplied directly to cell cultures. (A) Typical ROS assay after 72 h in HL. Differences in sensitivity to ROS are readily visible from the color of the culture. The dilution series of ROS-generating reagents were distributed across two 24-well plates with control cultures on each and the photo is a composite arrangement of the wells. Differential relative biomass accumulation ($\%A_{750}$) in response to increasing concentrations of rose bengal (B, E), methylviologen (C, F) and H_2O_2 (D, G) are shown representatively for wild type, *VHL*^{R}*-S4* and *VHL*^{R}*-S9*. Cells were grown and analyzed in LL (B, C, D) and HL (A, E, F, G). Values are means of $n=3-10$ per data point. The dashed lines indicate the 50% level of biomass relevant to the I_{50} determinations. The standard errors of the I_{50} value are shown in Table 2.

expression of APX [36] or double-antisense mutants lacking APX and catalase in higher plants [37], have not produced a strong "gain-of-function" phenotype comparable to *VHL*^{R} mutants. Furthermore, there is precedence for abiotic stress pathways converging at key regulatory genes as has been shown in drought and cold stress [38], however, manipulation of such genes normally had a growth penalty [39]. Until now, it has not been clear whether the physiological basis of the very high light resistant phenotype of the *Chlamydomonas reinhardtii VHL*^{R} mutants is primarily associated with alterations in photochemical processes, photoprotection or a combination of both [26,27].

It has now become obvious for the first time from our detailed investigation of the state of the photosynthetic reactions that the *VHL*^{R} phenotype is correlated with enhanced tolerance to reactive oxygen species. First, it can be ruled out that any of the four *VHL*^{R} mutations specifically affects accumulation of antennae, light-harvesting chlorophylls and photosystem complexes, or that alterations in electron transfer and photosystem function could be the primary basis for VHL resistance (Table 3). Second, the fact that PSII and PSI function and redox states are similar in the *VHL*^{R} mutants and in wild type suggests that there is not a reduced potential for ROS generation by

Table 2
Inhibitory effects of ROS on biomass accumulation in low and high light of VHL^R mutants compared to wild type (WT) and L^*

Genotype	I_{50} [μM]					
	Rose bengal ($^1O_2^*$)		Methylviologen (O_2^-)		H_2O_2	
	LL	HL	LL	HL	LL	HL
WT	0.57±0.15	0.27±0.10	0.11±0.02	0.11±0.02	490±30	450±70
VHL^R-S4	0.84±0.07	0.66±0.10	0.16±0.01	0.19±0.01	1090±50	470±80
VHL^R-S9	1.11±0.19	0.80±0.05	0.18±0.03	0.26±0.06	970±60	570±80
*L**	0.95±0.10	0.31±0.04	0.11±0.02	0.09±0.04	680±100	390±60
VHL^R-L4	1.12±0.19	0.84±0.04	0.13±0.03	0.29±0.11	930±80	600±50
VHL^R-L30	0.90±0.18	0.71±0.05	0.06±0.02	0.21±0.05	810±70	520±50

Singlet oxygen ($^1O_2^*$) and superoxide (O_2^-) levels were increased indirectly by adding rose bengal (RB) or methylviologen (MV), respectively, whereas additional hydrogen peroxide (H_2O_2) was supplied directly to cell cultures. The I_{50} values±standard errors represent the average concentrations of RB, MV or H_2O_2 causing 50% inhibition of growth (see Fig. 8). $n=3-10$ experiments.

the photosystems or an obvious change in the redox state of the PQ pool or lumenal pH (as inferred from NPQ measurements) that could lead to a more rapid or greater induction of photoprotective mechanism(s). An enhanced capacity for ROS detoxification is therefore the more likely mechanism for resistance to light stress.

The four VHL^R mutants capable of growing under light intensities lethal to wild type are also capable of growing in concentrations of ROS lethal to wild type. Photosynthetic growth in very high light will almost certainly be accompanied by high potential for ROS formation in the chloroplast, demanding high capacity for controlling ROS levels. Alternative explanations for ROS control in VHL^R mutants are that they have elevated capacity for ROS detoxification, that they may generate less ROS than wild type or a combination of both. This is corroborated by decreased superoxide anion and H_2O_2 accumulation within the first hour of very high light exposure in *VHL^R-S9*. The other three VHL^R mutants tested had similar levels of cumulative superoxide and H_2O_2 production compared to wild type after up to 1 h of VHL, confirming that different mechanisms of photoprotection are being enhanced in the different VHL^R mutants. While still conferring ROS tolerance, in these three mutants, there is either control of accumulation of ROS species other than superoxide anions, the control of superoxide levels occurs after 1 h of VHL or the light resistance may operate through enhanced repair or shielding of ROS targets in the cell.

The analysis of zeaxanthin-mediated photoprotection [26] provides further indirect evidence for enhanced ROS scavenging capacity under very high light. It has been shown that only few zeaxanthin molecules are needed for NPQ photoprotection [40]. In HL, NPQ was already induced to maximum levels in the four VHL^R mutants, yet 5-fold higher zeaxanthin levels are found in VHL^R mutants in VHL without further increasing NPQ. This excess zeaxanthin likely represents a "free" pool that has been proposed to act as antioxidant in thylakoids [4,41].

However, mechanisms other than zeaxanthin alone must be considered for enhanced resistance to methylviologen, rose bengal and hydrogen peroxide as these experiments were done at HL (Fig. 8) when wild type and corresponding VHL^R mutants had similar levels of zeaxanthin [26]. Moreover, differences in resistance to ROS-generating reagents persist in the absence of zeaxanthin in low light in both wild type and VHL^R mutants (Fig. 8). Furthermore, the primary function of zeaxanthin is quenching of ^{3}Chl and $^1O_2^*$, the latter a product of rose bengal. Thus, as noted by [5], it would certainly contribute to the enhanced resistance to ROS. However, zeaxanthin would only provide limited protection from superoxide and H_2O_2 formed at PSI, or by added MV which interacts with PSI to produce superoxide

Table 3
Summary of changes in photoprotective and photosynthetic properties of VHL^R mutants in very high light (VHL)

Genotype	Resistance to VHL	Resistance to ROS (HL)	Zeaxanthin levels	PSII repair (D1 synthesis)	Accumulation of photosystem and antenna proteins	Active PSII and PSI reaction centers	PSI oxidation and reduction
wild type	no	no	>[a]	Slow	<<	<<	<<
VHL^R-S9	yes	3×	>>	Fast	<	<	<
VHL^R-S4	yes	3×	>>	Nd	<	<	<
*L**	no	no	>[a]	Slow	<	<	<
*VHL^R-L**	yes	2.5×	>>	Fast	<	<	<

The analyses of mutants derived from wild type (*VHL^R-S4*, *VHL^R-S9*) and from the PSII-impaired L^* strain (*VHL^R-L**) were principally performed on VHL grown or exposed cells. As exception, ROS resistance was assessed in high light (HL) grown cells, and maximum resistance levels are presented. All other properties were evaluated relative to LL grown wild type or L^* controls. <, indicates the relative decrease following VHL treatments compared to LL. >, indicates the relative increase of zeaxanthin compared to LL.

[a] Zeaxanthin levels of HL grown cells. nd, not determined.

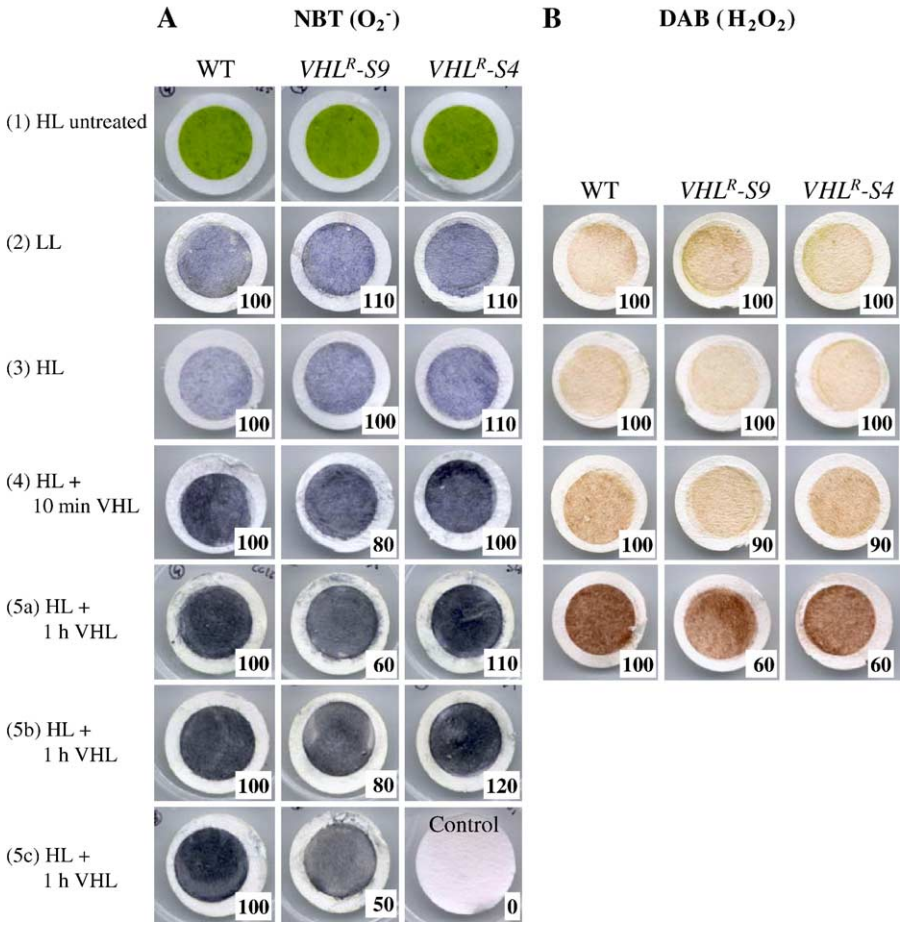

Fig. 9. Differential staining for accumulation of (A) superoxide anion with nitroblue tetrazolium (NBT) and (B) H_2O_2 with 3,3′ diaminobenzidine (DAB) of wild type (WT), *VHL^R-S9* and *VHL^R-S4* during different light treatments. Equal amounts of cells (biomass A_{750}) were deposited onto filter discs (1) and moistened with medium containing 1 mM NBT or 5 mM DAB. Following NBT and DAB treatment, pigments were bleached from the cells with acetone to compare levels of the dark blue formazan precipitate due to reduction of NBT by O_2^- and the reddish-brown polymerization product of DAB due to interaction with H_2O_2. Images from ROS staining of cells adapted to growth in LL (2), HL (3) or HL grown cells shifted to VHL for 10 min (4) or 1 h (5). Independent replicates are shown for NBT staining after 1h in VHL (5a–c). As a control, a filter without cells was treated to demonstrate that NBT (5c) or DAB (not shown) staining is solely dependent on the metabolic activity of the cells. Staining intensities were assessed semi-quantitatively by densitometry and are shown for each treatment as percentage of the equivalent wild type sample which was normalized to 100%.

anions and ultimately H_2O_2 [42]. Therefore, the reduced accumulation of superoxide anions and H_2O_2 in *VHL^R-S9* and the resistance to MV as well as hydrogen peroxide of many *VHL^R* mutants argue for enhanced activities of Mehler reactions and/or antioxidants such as ascorbate, which directly detoxify superoxide and contribute to the reduction of α-tocopherol and catalysis of H_2O_2 by ascorbate peroxidase [43]. It seems as if at least two modes of enhanced ROS detoxification operate in *VHL^R* mutants, namely ROS scavenging and zeaxanthin-dependent photoprotection. A third possibility to explain ROS resistance is faster or more efficient repair of ROS induced damage. This strongly implies that the *VHL^R* mutations affect genes above the structural level of individual components in the known ROS detoxification pathways. The identification of one or more *VHL^R* gene(s), which is the aim of work currently in progress, will add further understanding of the very high light resistance mechanisms.

VHL^R mutations in *Chlamydomonas reinhardtii* are distinctive in that they are a gain-of-function having arisen from natural selection pressure under full sunlight intensities rather than from mutagenesis and genetic manipulations. No single change, to either antenna size or to electron transport and function of PSII and PSI, provides mechanistic explanations for the *VHL^R* phenotype. Remarkably, not one of over 30 *VHL^R* mutants differed in PSII activity. Thus, more likely causes for the *VHL^R* phenotype are higher levels of protection from photo-oxidative stress mediated by elevated levels of zeaxanthin, higher rates of D1 synthesis and lower levels of ROS, particularly in *VHL^R-S9*. Yet, this increased tolerance to ROS and excess light has occurred without any obvious growth penalty at low or high irradiances, indicating that the underlying adaptations in *VHL^R* mutants do not demand extensive resources nor do they confer tolerance by generally impairing processes vital for photosynthetic productivity. The lack of photosynthetic

impairment as a mechanistic basis for the VHL^R phenotype among the large number of mutants furthermore suggests that selection pressure under very high light generally favors changes in processes that protect against oxidative stress.

Acknowledgements

We are grateful for prior support of this project in the laboratory of Drs. John Boynton and Nick Gillham at Duke University. This study was supported by Australian Research Council grants to B. F. (F100105701, DP0344313) and B. J. P. (DP0343160) and by the U.S. Department of Energy grant DE-FG05-89ER14005 to C. B. O.

References

[1] G. Öquist, N.P.A. Huner, Photosynthesis of overwintering evergreen plants, Annu. Rev. Plant Biol. 54 (2003) 329–355.
[2] X.P. Li, O. Björkman, C. Shih, A.R. Grossman, M. Rosenquist, S. Jansson, K.K. Niyogi, A pigment-binding protein essential for regulation of photosynthetic light harvesting, Nature 403 (2000) 391–395.
[3] K.K. Niyogi, Photoprotection revisited: genetic and molecular approaches, Annu. Rev. Plant Physiol. Plant Mol. Biol. 50 (1999) 333–359.
[4] M. Havaux, Carotenoids as membrane stabilizers in chloroplasts, TIPS 3 (1998) 147–151.
[5] I. Baroli, A.D. Do, T. Yamane, K.K. Niyogi, Zeaxanthin accumulation in the absence of a functional xanthophyll cycle protects *Chlamydomonas reinhardtii* from photooxidative stress, Plant Cell 15 (2003) 992–1008.
[6] E. Baena-Gonzalez, E.M. Aro, Biogenesis, assembly and turnover of photosystem II units, Phil. Trans. R. Soc. London, B 357 (2002) 1451–1459.
[7] J.M. Anderson, Y.I. Park, W.S. Chow, Unifying model for the photoinactivation of Photosystem II in vivo under steady-state photosynthesis, Photosynth. Res. 56 (1998) 1–13.
[8] H.Y. Lee, Y.N. Hong, W.S. Chow, Photoinactivation of photosystem II complexes and photoprotection by non-functional neighbours in *Capsicum annuum* L. leaves, Planta 212 (2001) 332–342.
[9] J.-D. Rochaix, N. Fischer, M. Hippler, Chloroplast site-directed mutagenesis of photosystem I in *Chlamydomonas*: electron transfer reactions and light sensitivity, Biochimie 82 (2000) 635–645.
[10] C. Barth, G.H. Krause, K. Winter, Responses of photosystem I compared with photosystem II to high-light stress in tropical shade and sun leaves, Plant Cell Environ. 24 (2001) 163–176.
[11] E. Hideg, T. Kalai, K. Hideg, I. Vass, Do oxidative stress conditions impairing photosynthesis in the light manifest as photoinhibition? Philos. Trans. R. Soc. London, B 355 (2000) 1511–1516.
[12] E. Hideg, I. Vass, Singlet oxygen is not produced in photosystem II under photoinhibitory conditions, J. Photochem. Photobiol. 62 (1995) 949–952.
[13] K. Brettel, Electron transfer and arrangement of the redox cofactors in photosystem I, Biochim. Biophys. Acta 1318 (1997) 322–373.
[14] T. Pfannschmidt, A. Nilsson, J.F. Allen, Photosynthetic control of chloroplast gene expression, Nature 397 (1999) 625–628.
[15] G. Forti, A. Furia, P. Bombelli, G. Finazzi, In vivo changes of the oxidation-reduction state of NADP and of the ATP/ADP cellular ratio linked to the photosynthetic activity in *Chlamydomonas reinhardtii*, Plant Physiol. 132 (2003) 1464–1474.
[16] J.-D. Rochaix, Genetics of the biogenesis and dynamics of the photosynthetic machinery in eukaryotes, Plant Cell 16 (2004) 1650–1660.
[17] K. Asada, The water–water cycle in chloroplasts: scavenging of active oxygens and dissipation of excess photons, Annu. Rev. Plant Physiol. Plant Mol. Biol. 50 (1999) 601–639.
[18] O. Oswald, T. Martin, P.J. Dominy, I.A. Graham, Plastid redox state and sugars: interactive regulators of nuclear-encoded photosynthetic gene expression, Proc. Natl. Acad. Sci. U. S. A. 98 (2001) 2047–2052.
[19] C.H. Foyer, G. Noctor, Redox sensing and signalling associated with reactive oxygen in chloroplasts, peroxisomes and mitochondria, Physiol. Plant. 119 (2003) 355–364.
[20] B.J. Pogson, K.K. Niyogi, O. Björkman, D. DellaPenna, Altered xanthophyll compositions adversely affect chlorophyll accumulation and nonphotochemical quenching in *Arabidopsis* mutants, Proc. Natl. Acad. Sci. U. S. A. 95 (1998) 13324–13329.
[21] P.B. Heifetz, A. Lers, D.H. Turpin, N.W. Gillham, J.E. Boynton, C.B. Osmond, dr and spr/sr mutations of *Chlamydomonas reinhardtii* affecting D1 protein function and synthesis define two independent steps leading to chronic photoinhibition and confer differential fitness, Plant Cell Environ. 20 (1997) 1145–1157.
[22] K. Satoh, in: K. Satoh, N. Murata (Eds.), Stress Responses of Photosynthetic Organisms, Elsevier Science, Amsterdam, 1998, pp. 3–14.
[23] Alía, Y. Kondo, A. Sakamoto, H. Nonaka, H. Hayashi, P.P. Saradhi, T.H.H. Chen, N. Murata, Enhanced tolerance to light stress of transgenic *Arabidopsis* plants that express the codA gene for a bacterial choline oxidase, Plant Mol. Biol. 40 (1999) 279–288.
[24] K. Shimogawara, S. Fujiwara, A. Grossman, H. Usuda, High-efficiency transformation of *Chlamydomonas reinhardtii* by electroporation, Genetics 148 (1998) 1821–1828.
[25] P. Müller-Moulé, T. Golan, K.K. Niyogi, Ascorbate-deficient mutants of *Arabidopsis* grow in high light despite chronic photooxidative stress, Plant Physiol. 134 (2004) 1163–1172.
[26] B. Förster, C.B. Osmond, J.E. Boynton, Very high light resistant mutants of *Chlamydomonas reinhardtii*: responses of Photosystem II, nonphotochemical quenching and xanthophyll pigments to light and CO_2, Photosynth. Res. 67 (2001) 5–15.
[27] B. Förster, C.B. Osmond, J.E. Boynton, N.W. Gillham, Mutants of *Chlamydomonas reinhardtii* resistant to very high light, J. Photochem. Photobiol., B 48 (1999) 127–135.
[28] E.H. Harris, The Chlamydomonas Source Book, Academic Press, San Diego, 1989.
[29] R.J. Porra, W.A. Thompson, P.E. Kriedemann, Determination of accurate extinction coefficients and simultaneous equations for assaying chlorophylls a and b extracted with four different solvents: verification of the concentration of chlorophyll standards by atomic absorption spectroscopy, Biochim. Biophys. Acta 975 (1989) 384–394.
[30] Z.S. Kolber, O. Prásil, P.G. Falkowski, Measurements of variable chlorophyll fluorescence using fast repetition rate techniques: defining methodology and experimental protocols, Biochim. Biophys. Acta 1367 (1998) 88–106.
[31] A. Lardans, N.W. Gillham, J.E. Boynton, Site-directed mutations at residue 251 of the photosystem II D1 protein of *Chlamydomonas* that result in a nonphotosynthetic phenotype and impair D1 synthesis and accumulation, J. Biol. Chem. 272 (1997) 210–216.
[32] A. Lardans, B. Förster, O. Prásil, P.G. Falkowski, V. Sobolev, M. Edelman, C.B. Osmond, N.W. Gillham, J.E. Boynton, Biophysical, biochemical, and physiological characterization of *Chlamydomonas reinhardtii* mutants with amino acid substitutions at the Ala(251) residue in the D1 protein that result in varying levels of photosynthetic competence, J. Biol. Chem. 273 (1998) 11082–11091.

[33] M. Shapira, A. Lers, P.B. Heifetz, V. Irihimovitz, C.B. Osmond, N.W. Gillham, J.E. Boynton, Differential regulation of chloroplast gene expression in *Chlamydomonas reinhardtii* during photoacclimation: Light stress transiently suppresses synthesis of the Rubisco LSU protein while enhancing synthesis of the PS II D1 protein, Plant Mol. Biol. 33 (1997) 1001–1011.

[34] W.S. Chow, A.B. Hope, J.M. Anderson, Further studies on quantifying photosystem II in-vivo by flash-induced oxygen yield from leaf discs, Aust. J. Plant Physiol. 18 (1991) 397–410.

[35] B. Förster, P.B. Heifetz, A. Lardans, J.E. Boynton, N.W. Gillham, Herbicide resistance and growth of D1 Ala(251) mutants in *Chlamydomonas*, Z. Naturforsch., C 52 (1997) 654–664.

[36] I. Murgia, D. Tarantino, C. Vannini, M. Bracale, S. Carravieri, C. Soave, *Arabidopsis thaliana* plants overexpressing thylakoidal ascorbate peroxidase show increased resistance to paraquat-induced photooxidative stress and to nitric oxide-induced cell death, Plant J. 38 (2004) 940–953.

[37] L. Rizhsky, E. Hallak-Herr, F. Van Breusegem, S. Rachmilevitch, J.E. Barr, S. Rodermel, D. Inze, R. Mittler, Double antisense plants lacking ascorbate peroxidase and catalase are less sensitive to oxidative stress than single antisense plants lacking ascorbate peroxidase or catalase, Plant J. 32 (2002) 329–342.

[38] J.Z. Zhang, R.A. Creelman, J.-K. Zhu, From laboratory to field. Using information from *Arabidopsis* to engineer salt, cold, and drought tolerance in crops, Plant Physiol. 135 (2004) 615–621.

[39] S.J. Gilmour, A.M. Sebolt, M.P. Salazar, J.D. Everard, M.F. Thomashow, Overexpression of the *Arabidopsis* CBF3 transcriptional activator mimics multiple biochemical changes associated with cold acclimation, Plant Physiol. 124 (2000) 1854–1865.

[40] A. Gilmore, Xanthophyll cycle-dependent nonphotochemical quenching in Photosystem II: mechanistic insights gained from *Arabidopsis thaliana* L. mutants that lack violaxanthin deepoxidase activity and/or lutein, Photosynth. Res. 67 (2001) 89–101.

[41] M. Havaux, L. Dall'Osto, S. Cuine, G. Giuliano, R. Bassi, The effect of zeaxanthin as the only xanthophyll on the structure and function of the photosynthetic apparatus in *Arabidopsis thaliana*, J. Biol. Chem. 279 (2004) 13878–13888.

[42] Y. Nishiyama, H. Yamamoto, S.I. Allakhverdiev, M. Inaba, A. Yokota, N. Murata, Oxidative stress inhibits the repair of photodamage to the photosynthetic machinery, EMBO J. 20 (2001) 5587–5594.

[43] C.H. Foyer, J. Harbinson, in: H.A. Frank, A.J. Young, G. Britton, R.J. Cogdell (Eds.), The Photochemistry of Carotenoids, Kluwer Academic, Dordrecht, 1999, pp. 305–325.